IHJPAS. 36 (4) 2023

Ibn Al-Haitham Journal for Pure and Applied Sciences
Journal homepage: jih.uobaghdad.edu.iq

Enhancing Gas Sensing Performance of TiO_2-ZnO nanostructures: Effect of ZnO Concentration

Israa Abdul Kareem *
Department of Physics, College of Sciences for Women, University of Baghdad, Baghdad, Iraq.

Hind Fadhil Oleiwi
Department of Physics,College of Sciences for Women, University of Baghdad, Baghdad, Iraq.

***Corresponding Author:** Israa.abdulkareem1204a@csw.uobaghdad.edu.iq

Article history: Received 4 January 2023, Accepted 12 February 2023, Published in October 2023.

doi.org/10.30526/36.4.3173

Abstract

Gas sensors based on titanium dioxide (TiO_2) and zinc oxide (ZnO) nanocomposites are considered as energy-saving devices that are utilized to find dangerous or harmful gases in an environment. The performance of nitrogen dioxide (NO_2) gas sensors has been improved by spin-coating a TiO_2 and TiO_2:ZnO nanocomposite with varying concentrations ($_{90}TiO_2$:$_{10}$ZnO, $_{70}TiO_2$:$_{30}$ZnO, and $_{50}TiO_2$:$_{50}$ZnO). To correlate structural properties with gas-sensing behavior, structural and morphological characterisation has been done using FESEM, XRD, and EDX. Without any ZnO-specific crystalline phase, TiO_2 X-ray diffraction was found to be indexed in the anatase crystalline structure. The ZnO is synthesized in the wurtzite phase with (002) orientation and has a smooth surface, according to the morphologies and crystalline structure of the films, which also indicated the presence of ZnO components with various crystallite sizes and lattice strains. Responses to NO_2 are increased by low ZnO content. Additionally, at the average operating temperature of 250 ^oC, TiO_2:ZnO shows good response.

Keywords: TiO_2:ZnO nanocomposite, spin-coating technique, defect, NO_2 gas sensor.

1. Introduction

Increased environmental contamination and, as a result, increased health concerns have become one of the most pressing issues of our day. Different gases are also commonly employed in industrial applications. Human health is directly affected by this condition because of their utility, the integration of smart gadgets made for the benefit of mankind into our everyday lives has grown in popularity over the years [1]. As smart sensors, sensors made using microtechnologies offer benefits in terms of cost, compactness, and sensitivity. Gas detection devices, in this perspective, are crucial for a variety of applications, including monitoring gas buildup, medical

diagnostics, food quality assurance, and the safety of industrial or residential activities [2, 3]. The characteristics of the sensing material have an impact on sensor specifications including sensitivity, selectivity, response, and recovery times. By fabricating gas sensors from semiconductor oxides with highly sensitive to gases, these limitations can be overcome [4-6]. Metal oxide semiconductors including TiO_2 and ZnO are important materials and have been widely studied [7, 8]. Because of their chemical stability, low cost, non-toxic semiconductor material, and photocatalytic efficiency properties [9-11]. Titanium dioxide (TiO_2) has proven distinctive and improved physical and chemical properties crucial for applications like photocatalysis [12], water splitting, and sensing when combined with ZnO (creating heterostructure) [13]. The two most commonly used sensing materials are TiO_2 and ZnO. In comparison to TiO_2, ZnO has a smaller band gap (3.37 eV at room temperature), valence band potential, exciton binding energy, and electron mobility (0.1-4 cm^2.V.s) [14]. It has thus been investigated for any possible dangers. It might be employed in applications involving gas sensing. Conduction band holes from TiO_2 in the valence band (VB) might easily transfer to the valence band (VB) of ZnO, and vice versa. Numerous applications may be made use of this ease of transmission between TiO_2 and ZnO. Furthermore, ZnO is an inherently n-type semiconductor with a band gap of 3.37 eV and a significant exciton binding energy of 60 meV [15].

In the current study, a low-cost synthesis of amorphous TiO_2: ZnO with different concentrations of ZnO was prepared by spin-coating technique and study the influence of the concentration of ZnO on the properties of the film and examined the performance structure as NO_2 gas sensor.

2. Materials and Methods

All chemicals were of analytical grade and used without additional purification. Titanium dioxide (TiO_2 99.5%) and zinc oxide (ZnO 99.8%) powder were used. Deionized water (DI) was used to clean and wash soda-lime glass plates (20 x 20 x 2) mm^3, which were then washed with acetone and 2-propanol in a sonication for 18 minutes. The substrate was then dried in an oven to ensure that all surface impurities were eliminated. Solutions containing 20.0 g/L of TiO_2 and TiO_2:ZnO nanocomposite at varying concentrations ($_{90}TiO_2$:$_{10}$ZnO, $_{70}TiO_2$:$_{30}$ZnO, and $_{50}TiO_2$:$_{50}$ZnO) were created. The mixtures were constantly stirred until uniform and white in color. After that, glass substrates were coated with TiO_2 and a TiO_2:ZnO precursor solution using the spin-coating process at a 3000 rpm deposit speed. The films were heated at 100 °C for 10 minutes after each layer of coating to eliminate organic compounds from the structure. This procedure was repeated until the appropriate thickness was reached (up to 3 layers). The coated glass substrates were then annealed for one hour at 300 ^oC.

3. Characterization

The elemental mapping was determined using a Field Emission Scanning Electron Microscope (FESEM) (model TESCAN MIRA3 FRENCH) connected to an EDX device to get cross-sectional pictures and top views of the samples. The structural characteristics of prepared samples were determined using the X-ray diffraction technique (XRD 6000) (SHIMADZU Japan). We employed Hall effect measurements to learn about the semiconductor's quality, the carrier's concentration and mobility, and the distance factor at room temperature, as a device (HMS-3000 equipped with ECOPIA Co. Korea), was used to determine the charge carriers and compute the RH coefficient.

4. Results and Discussion

Figure 1 shows top-view FESEM images with different scales bare for TiO_2, and TiO_2:ZnO nanocomposite with different concentrations ($_{90}$ TiO_2:$_{10}$ZnO, $_{70}TiO_2$:$_{30}$ZnO, and $_{50}TiO_2$:$_{50}$ZnO). These photos demonstrated highly homogeneous surfaces with diameters ranging from 50.08, 48.97, 40.55, and 31.58nm, respectively, this means that all TiO_2:ZnO oxide materials that have been examined have nonmetric particles that are less than 100 nm. All samples contain almost spherically shaped particles with a high tendency to agglomerate, according to the FESEM images. Field Emission Scanning Electron Microscope (FESEM) images show that the ZnO concentration has a considerable impact on the final nanocomposite's shape. These findings are in agreement with those of other researchers [16].

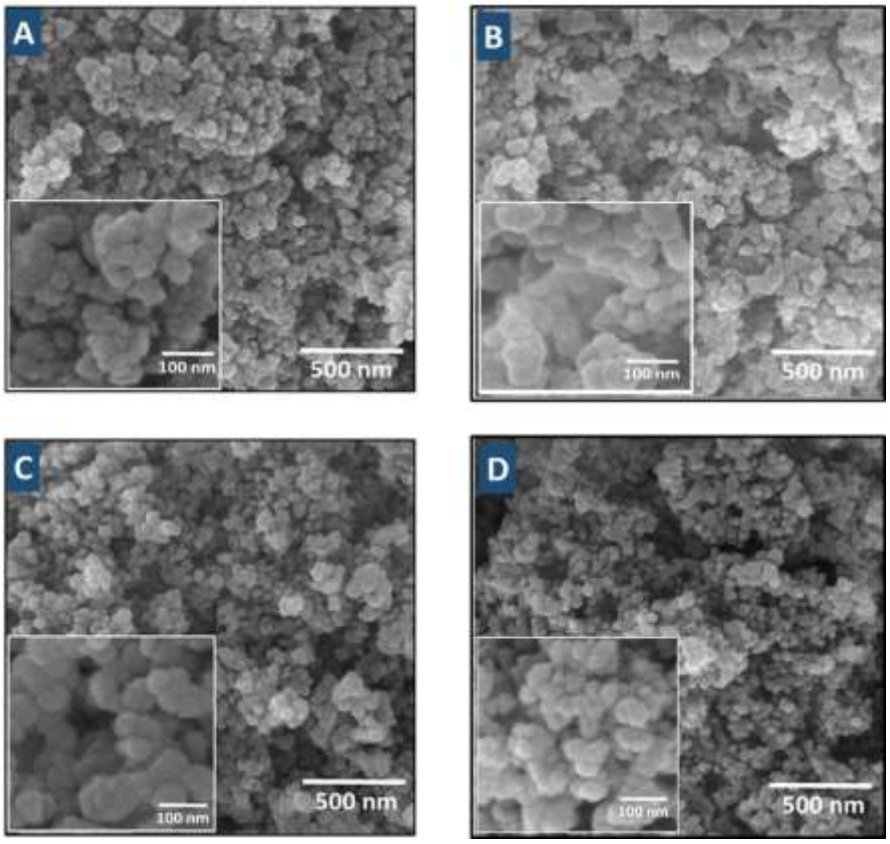

Figure 1. FESEM images show the different scales of (A) TiO_2, (B) $_{90}$ TiO_2:$_{10}$ZnO, (C) $_{70}TiO_2$:$_{30}$ZnO, and (D) $_{50}TiO_2$:$_{50}$ZnO

To determine the correct quantity of materials contained in samples, chemical composition analysis is very necessary. Figure 2 explains Ti, O, and Zn elements in TiO_2 and $_{50}TiO_2$:$_{50}$ZnO using Energy dispersive X-ray spectroscopy (EDX) analysis linked with the FESEM device. This analysis shows that the atomic ratio of Ti is 40.10% and 26.63% for O for the TiO_2 sample. In addition, the atomic ratio for the $_{50}TiO_2$:$_{50}$ZnO sample was 23.99, 20.14, and 13.13% for T, O, and Zn respectively.

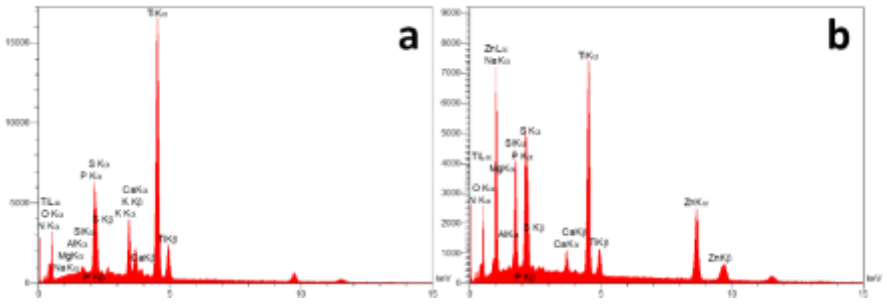

Figure 2. EDX spectrum of (a) TiO_2 and (b) $_{50}TiO_2{:}_{50}ZnO$ prepared using spin-coating technique

Fig 3 shows the results of an X-ray diffraction (XRD) analysis of the structural characteristics of TiO_2 and TiO_2: ZnO nanoparticles. The XRD patterns that were obtained for pure TiO_2 in this work are similar with the standard spectrum that has been recorded and is connected to the anatase phase (JCPDS No. 21-1272) TiO_2 has a tetragonal crystal structure, and its computed lattice parameters are (a=3.78A^o, c=9.504A^o). Moreover, it displays peaks at 2 values of 25.28 and 47.98, respectively, which correspond to (101) and (200).

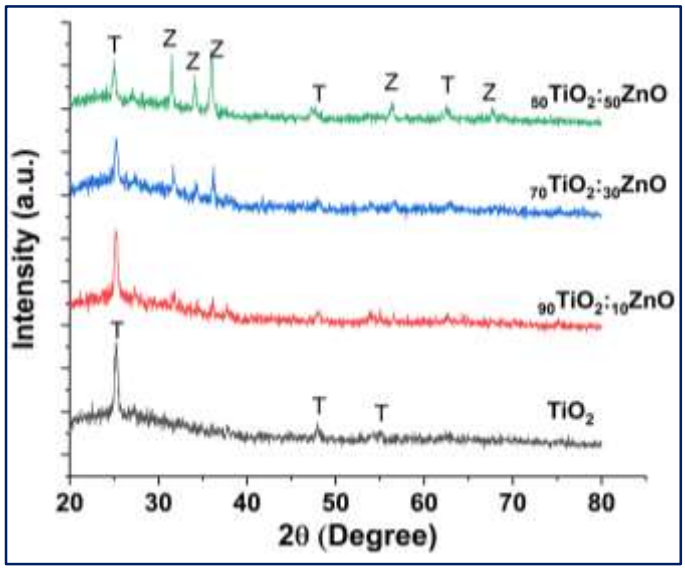

Figure 3. XRD patterns of TiO_2, $_{90}TiO_2{:}_{10}ZnO$, $_{70}TiO_2{:}_{30}ZnO$, and $_{50}TiO_2{:}_{50}ZnO$

The TiO_2 phase fraction will dramatically drop for $_{90}TiO_2{:}_{10}ZnO$, $_{70}TiO_2{:}_{30}ZnO$, and $_{50}TiO_2{:}_{50}ZnO$. It was found that the intensity of the distinctive anatase peak at 2 = 25.28 declines as TiO2 content decreases. In addition, it was found that crystalline structure of TiO2 is inhibited by the presence of ZnO. The findings from Chen et al., Tian et al., and Choi et al. [17-19] are in agreement with our findings. This behavior can only be explained by the fact that Zn^{2+} ions and Ti^{+4} ions respective radii are 0.042-0.074 nm and 0.06-0.09 nm [20, 21]. The crystalline TiO_2:ZnO structure of wurtzite (JCPDS No. 36-1451), however, exhibits reflections at values of 25.049, 31.54, 34.19, 36.03, 47.47, and 56.41 that correspond to (101), (100), (002), (101), (200), and (110). The lattice parameters of ZnO were estimated as (a=3.2493A^o,c = 5.207) [22]. There are no additional impurity peaks are detected, indicating the non-existence of other impurities.

The results of XRD analysis prove that ZnO concentrations affect the crystalline structure of the resulting binary oxide system.

Hall effect measurements at room temperature of TiO_2 and TiO_2:ZnO nanocomposite reveal the kind of majority charge carriers, carrier mobility, and electric charge density for all films. According to table 1, the concentration of carriers reduced as the concentration of ZnO, with exception of sample 70:30, and the mobility of carriers increased. The primary causes of changes in mobility and concentration carriers are growth in grain boundaries and the emergence of crystal lattice distribution, which causes an increase in the scattering center for impurities. When ZnO is added to TiO_2 NPs, the mobility carrier increases, which might improve the crystallinity of films.

Table 1. The concentration and mobility carriers

Sample	μ_H ($cm^2/V.sec$)	$n*10^{12}$ (cm^{-3})	Type
TiO_2	14.8	8.90	n-type
$_{90}TiO_2:_{10}ZnO$	15.1	9.21	n-type
$_{70}TiO_2:_{30}ZnO$	14.4	10.7	n-type
$_{50}TiO_2:_{50}ZnO$	13.5	15.58	n-type

The gas sensing characteristics of pure TiO_2 and TiO_2:ZnO films on a glass substrate with various concentration ratios are investigated as a function of operating temperature and (NO_2) gas exposure time. The oxidation and reduction process results in a change in gas sensor resistance (decrease or increase). **Figures 4-7** show the resistance changes in TiO_2, ZnO, and TiO_2:ZnO samples. An increase in resistance when the films are exposed to NO_2 gas (Gas ON), then a decrease in resistance when the gas is turned off (Gas OFF). The following reason for this behavior: NO_2 gas molecules are adsorbed on surfaces TiO_2, ZnO, and TiO_2:ZnO when exposed to the gas. The consumption of electrons by each NO_2 molecule during its reaction with the surface of TiO_2 and TiO_2:ZnO, leads to a reduction in conductivity and NO_2 molecules oxidized the surfaces and increase the surface resistance, which can be used for sensing NO_2 gas[9]. To determine the operating temperature of the sensor, where the operational temperature of a sensor is defined as the temperature at which its resistance remains constant. Changes in resistance are only influenced by the presence of a certain amount of gas of interest [10].

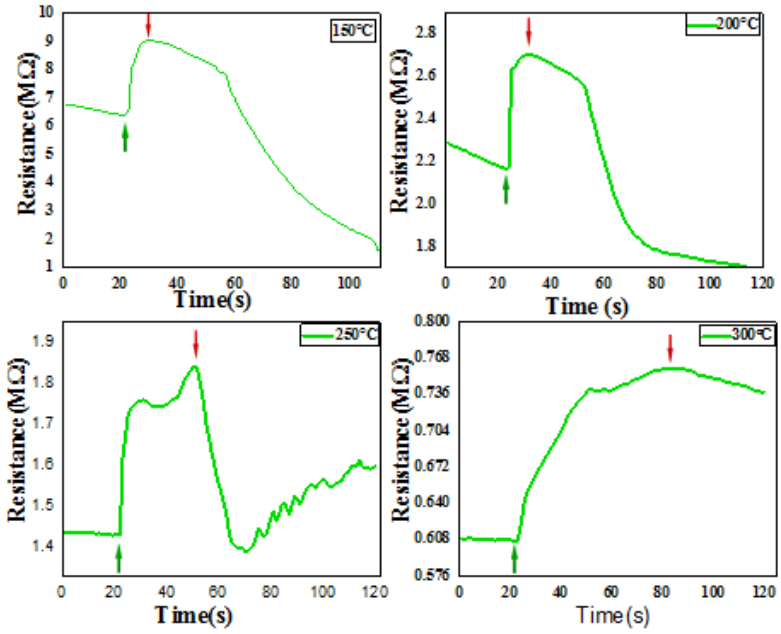

Figure 4. Resistance versus time for pure TiO_2

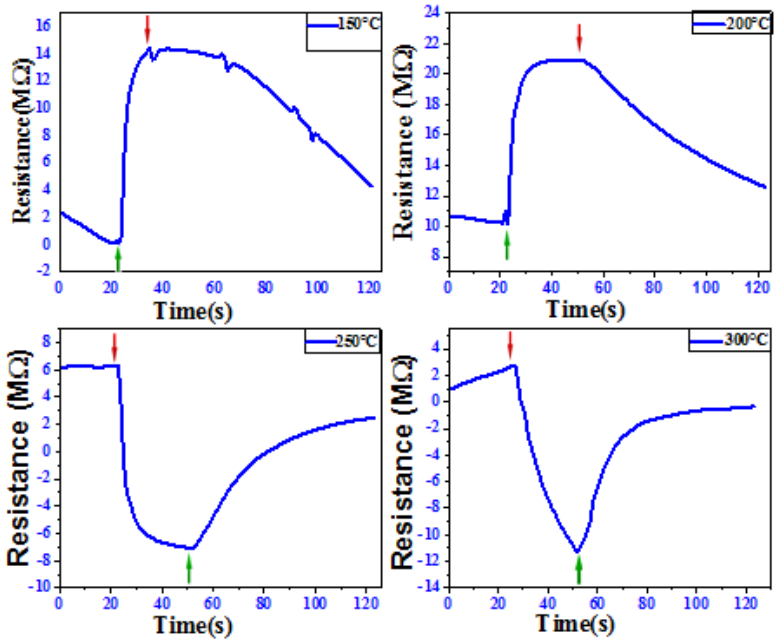

Figure 5. Resistance versus time for $_{90}TiO_2$:$_{10}ZnO$

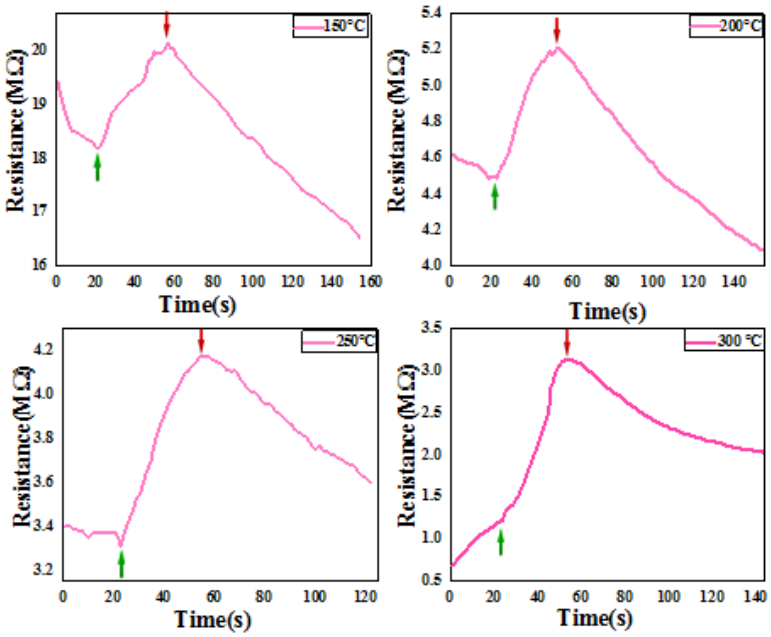

Figure 6. Resistance versus time for $_{70}TiO_2$:$_{30}ZnO$

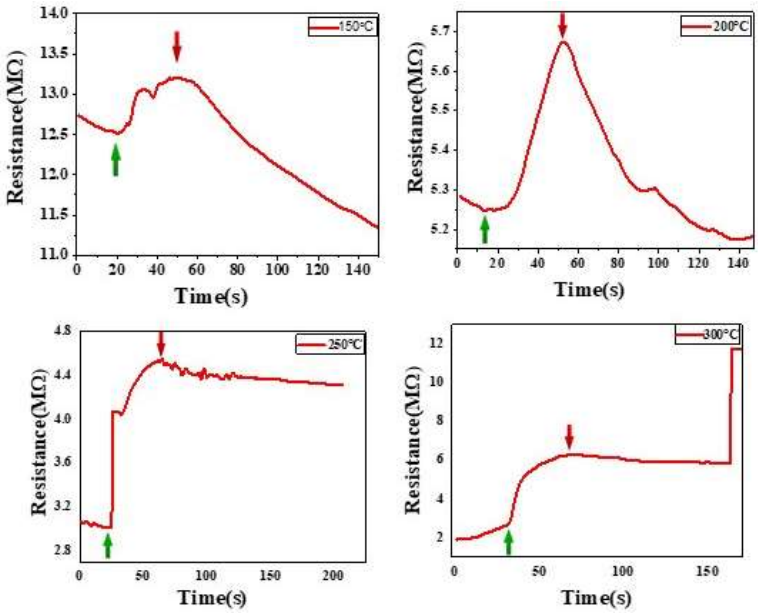

Figure 7. Resistance versus time for $_{50}TiO_2$:$_{50}ZnO$

Figures 8-10 show the response time and the sensitivity% with different operating temperatures of pure TiO_2 and TiO_2:ZnO thin films with different concentrations and the variation of response time and recovery time versus working temperature of pure TiO_2 and TiO_2:ZnO with different concentrations prepared through spin coating techniques respectively.

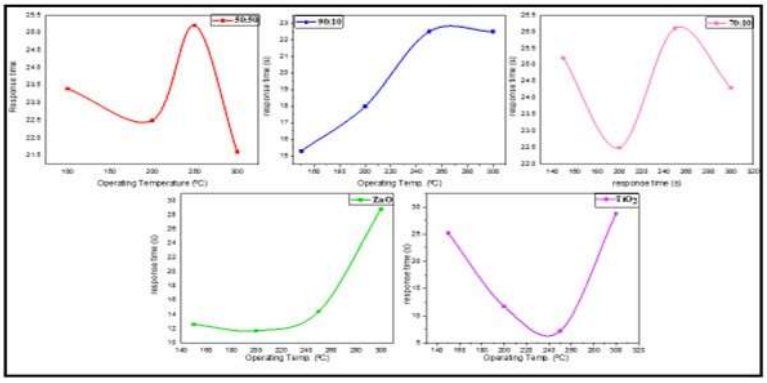

Figure 8. The variation of response time with the working temperature of TiO_2 and different concentrations of TiO_2:ZnO

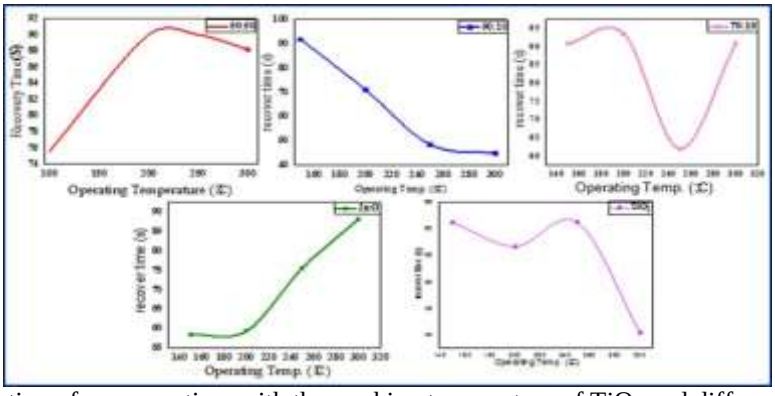

Figure 9. The variation of recovery time with the working temperature of TiO_2 and different concentrations of TiO_2:ZnO

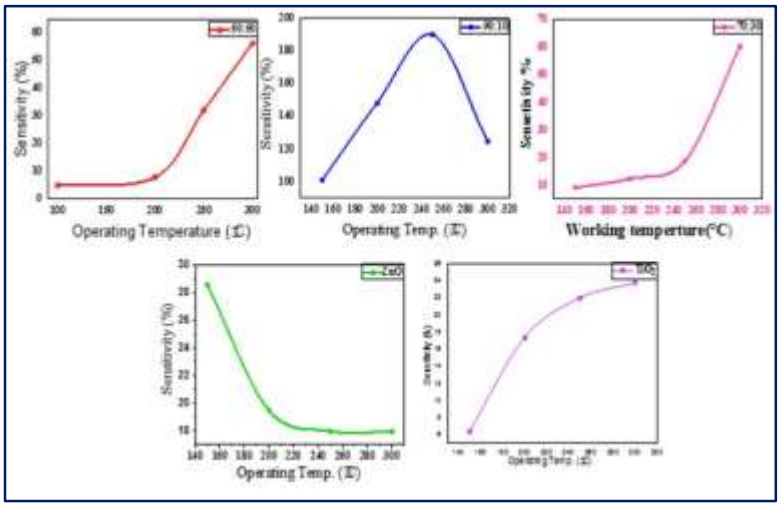

Figure 10. Sensitivity for TiO_2 and TiO_2:ZnO with different concentrations

Table 2 shows sensitivity%, Response, and Recovery time at different temperatures for TiO_2 and TiO_2:ZnO of samples prepared by spin coating. Temperatures of (150°C, 200°C, 250°C, and 300°C) were used to investigate gas sensitivity. At 300°C, it demonstrated the highest sensitivity for all samples except $_{90}TiO_2$:$_{10}$ZnO the highest sensitivity at 250°C. The highest sensitivity values are 190.06% for the $_{90}TiO_2$:$_{10}$ZnO sample prepared. Also, the electrical conductivity of

the material is high so the material takes a long time and the same conduct exists in $_{50}TiO_2$:$_{50}ZnO$ and $_{70}TiO_2$:$_{30}ZnO$ with the highest sensitivity of 56.48% and 60.39% respectively.

Table 2. Sensitivity%, Response, and Recovery time of different temperatures for pure TiO_2 and TiO_2:ZnO at different concentrations

Sample	Working Temperature (°C)	Sensitivity (%)	Response Time (s)	Recover Time (s)
TiO_2	150	28.57	12.6	58.5
	200	19.50	11.7	59.4
	250	17.99	14.4	75.6
	300	71.95	28.8	88.2
$_{90}TiO_2$:$_{10}ZnO$	150	100.85	15.3	91.8
	200	148.40	18	71.1
	250	190.03	22.5	48.6
	300	124.81	22.5	45
$_{70}TiO_2$:$_{30}ZnO$	150	9.16	25.2	90.9
	200	12.45	22,5	93.6
	250	18.89	26,1	62.1
	300	60.4	24,3	90.9
$_{50}TiO_2$:$_{50}ZnO$	150	5.02	23.4	75.6
	200	7.95	22.5	90
	250	32.21	25.2	90
	300	56.48	21.6	88.2

5. Conclusion

The spin-coating technique was used to deposit very homogeneous TiO_2 nanoparticles with varying ZnO concentrations on a glass substrate. Field Emission Scanning Electron Microscope (FESEM) images revealed that samples had a smooth surface and a spherical shape. All samples contained symmetric ZnO wurtzite hexagonal structures, which was demonstrated by the X-ray diffraction investigation and suggested the presence of a highly crystalline ZnO nanostructure. On pure TiO_2, ZnO, and TiO_2:ZnO materials, gas sensor measurements against NO_2 gas show that the optimal operating temperature is at 200°C and diminishes with rising temperatures over 300 °C. The mobility carrier rises when ZnO is added to TiO_2 NPs, which may enhance the crystallinity of films. The results indicate that NO_2 gas sensor performances improved due to an increase in the defect density and generate an impurity state within the energy band structure of ZnO which enhances the adsorption site. The main reason for the choice of this bilayer system is the different behavior of TiO_2 when the ZnO layer is deposited on the glass/TiO_2 film.

References

1. Zhang, Z., et al., Optimizing the gas sensing characteristics of Co-doped SnO2 thin film based hydrogen sensor. *Journal of Alloys and Compounds*, **2019**,*785*, 819-825.
2. Nakata, K. ; A. Fujishima, *TiO2 photocatalysis: Design and applications. Journal of photochemistry and photobiology C: Photochemistry Reviews*, **2012,** *13(3)*,169-189.
3. EGE, G.K.; Hüseyin, Y.; Garip G., A Gas Sensor Design and Heat Transfer Simulation with ZnO and TiO2 Sensing Layers. *MANAS Journal of Engineering*, **2021**, *9(1)*,37-44.

4. Lei, Y., Wireless 3D Nanorod Composite Arrays based High Temperature Surface-Acoustic-Wave Sensors for Selective Gas Detection through Machine Learning Algorithms. **2019**, *Univ. of Connecticut, Storrs, CT (United States)*.

5. Aadim, K.A. ;N.K. Abbas, Synthesis and fabrication of In2O3: CdO nanoparticles for NO2 Gas Sensor. *Baghdad Science Journal*, **2018**,15(3).

6. Kareem, S.M., *Cr2O3:* TiO2 Nanostructure Thin Film Prepared by Pulsed Laser Deposition Technique as NO2 Gas Sensor. *Baghdad Science Journal*, **2020**, *17*(1 (Suppl.)) 0329-0329.

7. Al-Awadi, S.S., et al., Optical and structural properties of titanium dioxide papered by dc magneto-sputtering as a NO2 gas sensor. *Iraqi Journal of Science*, **2020**, 2562-2569.

8. Al-Taa'y, W.A. ; Hasan, B.A. Design and Fabrication of Nanostructure TiO2 Doped NiO as A Gas Sensor for NO2 Detection. *Iraqi Journal of Science*, **2021**,4385-4396.

9. Padvi, M., et al., A critical review on design and development of gas sensing materials. *Engineered Science*, **2021**,*15*,20-37.

10. Tu, Y., et al., Light-addressable potentiometric sensors using ZnO nanorods as the sensor substrate for bioanalytical applications. *Analytical chemistry*, **2018**, *90(14)*, 8708-8715.

11. Shao, D., et al., High quality ZnO–TiO2 core–shell nanowires for efficient ultraviolet sensing. *Applied surface science*, **2014**, *314*, 872-876.

12. Giannakopoulou, T., et al., Optical and photocatalytic properties of composite TiO2/ZnO thin films. *Catalysis Today*, **2014**, *230*, 174-180.

13. Habib, M.A., et al., Synthesis and characterization of ZnO-TiO2 nanocomposites and their application as photocatalysts. *International Nano Letters*, **2013**,*3(1)*, 1-8.

14. Mang, A. ; Reimann, K.Band gaps, crystal-field splitting, spin-orbit coupling, and exciton binding energies in ZnO under hydrostatic pressure. *Solid state communications*, **1995**,*94(4*), 251-254.

15. Bhati, V.S.; Hojamberdiev, M.; Kumar, M.Enhanced sensing performance of ZnO nanostructures-based gas sensors: A review. *Energy Reports*, **2020**, *6*, 46-62.

16. Kheiri, F., et al., The microstructure, optical and gas sensing properties of bilayer TiO2/ZnO systems in terms of annealing temperature. *Materials Science in Semiconductor Processing*, **2021**, *121*,105462.

17. Choi, W.S., et al., Optical and structural properties of ZnO/TiO2/ZnO multi-layers prepared via electron beam evaporation. *Vacuum*, **2009**, *83(5)*, 878-882.

18. Tian, J., et al., Preparation and characterization of TiO2, ZnO, and TiO2/ZnO nanofilms via sol–gel process. *Ceramics International*, **2009**,*35(6)*, 2261-2270.

19. Khalili, S., et al., Investigation of the lattice defects density and optical characteristics for the anatase phase of titanium dioxide nanocrystalline films. *Applied Physics A*, **2019**, *125(9)*, 1-11.

20. Li, Z., et al., Resistive-type hydrogen gas sensor based on TiO2: A review. *International Journal of Hydrogen Energy*, **2018**, *43(45)*, 21114-21132.

21. Kusdianto, K., et al. ZnO-TiO2 nanocomposite materials: fabrication and its applications. in *IOP Conference Series: Materials Science and Engineering*. **2021.** IOP Publishing.

22. Viezbicke, B.D., et al., Evaluation of the Tauc method for optical absorption edge determination: ZnO thin films as a model system. *physica status solidi* (b), **2015**, *252(8)*,1700-1710.